agronomy

MDPI

Article

RTM Inversion through Predictive Equations for Multi-Crop LAI Retrieval Using Sentinel-2 Images

Michele Croci [1,2], Giorgio Impollonia [1,2], Andrea Marcone [1], Giulia Antonucci [1], Tommaso Letterio [3], Michele Colauzzi [1], Marco Vignudelli [4], Francesca Ventura [4], Stefano Anconelli [3] and Stefano Amaducci [1,2,*]

1 Department of Sustainable Crop Production (DI.PRO.VE. S.), Università Cattolica del Sacro Cuore, 29122 Piacenza, Italy
2 Remote Sensing and Spatial Analysis Research Center (CRAST), Università Cattolica del Sacro Cuore, 29122 Piacenza, Italy
3 Consorzio Bonifica CER, 40137 Bologna, Italy
4 Department of Agricultural and Food Sciences (DISTAL), Alma Mater Studiorum Università di Bologna, 40126 Bologna, Italy
* Correspondence: stefano.amaducci@unicatt.it

Abstract: Near-real-time, high-spatial-resolution leaf area index (LAI) maps would enable producers to monitor crop health and growth status, improving agricultural practices such as fertiliser and water management. LAI retrieval methods are numerous and can be divided into statistical and physically based methods. While statistical methods are generally subject to high site-specificity but possess high ease of implementation and use, physically based methods are more transferable, albeit more complex to use in operational settings. In addition, statistical methods need a large amount of data for calibration and subsequent validation, and this is only seldom feasible. Techniques based on predictive equations ($PE_{physical}$) represent a viable alternative, allowing the partial combination of statistical and physical methods merits while minimising their shortcomings. In this paper, predictive equation-based techniques were compared with four other methods: two radiative transfer model (RTM) inversion methods, one based on neural network (NNET) and one based on a look-up table (LUT), and two empirical methods (one using empirical models based on vegetation indices and in situ data and one based on empirical models found in the scientific literature). The methods were chosen based on common use. To evaluate the performance of the studied methods, the coefficient of determination (R^2), root mean square error (RMSE), and normalised root mean square error (nRMSE, %) between the estimates and in situ LAI measurements were reported. The best $PE_{physical}$ results, achieved by the OSAVI index (RMSE = 0.84 m^2 m^{-2}), provided better performance for LAI recovery than the NNET-based RTM inversions (0.86 m^2 m^{-2}) or the estimates made by LUT (0.94 m^2 m^{-2}). Furthermore, the best $PE_{physical}$ produced accuracies comparable to the best empirical model (RMSE = 0.71 m^2 m^{-2}), calibrated through in situ data, and similar to the best literature model (RMSE = 0.76 m^2 m^{-2}). These results indicated that $PE_{physical}$ can be used to recover LAI with transferability comparable to literature models.

Keywords: LAI; precision agriculture; empirical model; PROSAIL; LUT; predictive equation; NNET

Citation: Croci, M.; Impollonia, G.; Marcone, A.; Antonucci, G.; Letterio, T.; Colauzzi, M.; Vignudelli, M.; Ventura, F.; Anconelli, S.; Amaducci, S. RTM Inversion through Predictive Equations for Multi-Crop LAI Retrieval Using Sentinel-2 Images. *Agronomy* **2022**, *12*, 2835. https://doi.org/10.3390/agronomy12112835

Academic Editor: Yash Dang

Received: 30 September 2022
Accepted: 10 November 2022
Published: 13 November 2022

1. Introduction

Timely information on crop growth and health is increasingly important for developing strategic food policies and for supporting natural resource management [1–3]. Mapping crop biophysical parameters is essential in many applications of land surface monitoring [4,5]. Leaf Area Index (LAI), in particular, is of particular interest and the most studied among biophysical parameters. A key canopy structural variable, it is often used to model surface energy balance and crop productivity as well as study water and carbon balances from the soil–crop–atmosphere continuum [6–9]. For these reasons, at field scale, the availability of near real-time estimation of LAI would enable producers to monitor crop

health and growth status and improve agricultural practices' efficiency, such as fertiliser application and water management [1,10]. However, direct measurements of biophysical parameters are labour-intensive [11]. For this reason, the use of remote-sensing techniques involving satellites providing a high rate of revisit frequency, requiring limited labour, and enabling crop biophysical parameter measurement at different scales, is rapidly expanding [12]. Recently, several approaches have been developed to retrieve crop biophysical parameters through remote-sensing techniques. These techniques can be summarised into two main approaches [13,14]: (i) statistical approaches, which typically consist of relating the biophysical parameters to spectral data through linear or non-linear regression techniques (e.g., polynomial regressions or machine learning algorithms) and (ii) physical approaches using physically based radiative transfer models (RTMs) [15,16]. In statistical approaches, biophysical parameters are correlated with vegetation indices (VIs) that combine two or more spectral bands sensitive to the biophysical parameter of interest [17]. This technique enables enhancing the spectral characteristics of a specific vegetation property while minimising the background effects of soil, atmosphere [18–21], and sun-target-sensor geometry [22]. While the statistical approach has some advantages, including the ease of use in operational settings and their availability in the scientific literature [14], it also has several disadvantages. Models based on statistical approaches are known to have reduced transferability to conditions other than those in which they were developed [23,24] and require in situ data for their calibration. Therefore, the robustness of these models will depend on the amount, quality, and distribution of data, which are often very complex to collect in large numbers [25].

In contrast, the physical approaches using radiative transfer models (RTMs) are more robust for LAI retrieval, overcoming the problem of lack of transferability due to their ability to simulate radiative behaviour mechanistically. However, RTMs are more complex and require more computational cost in their calibration step compared with statistical approaches. RTMs model the spectral variation of the canopy reflectance using physical principles involving viewing and illumination geometry, biophysical and biochemical characteristics of leaves and canopy, and soil characteristics [16]. In literature, adequate results have been reported for LAI retrieval using the PROSAIL canopy reflectance model-a combination of the PROSPECT [26] and SAIL [27] models-as revised by Jacquemoud et al. [16]. The PROSAIL model does not directly produce estimates of a crop's biophysical parameters, but it does enable the generation of a spectral database that must subsequently be inverted using appropriate inversion strategies in order to retrieve the related biophysical parameters [28,29]. Available inversion techniques include Look Up Tables—LUT [30–32] and hybrid regression approaches based on machine learning algorithms, such as artificial neural networks (NNET) [33,34], which combine physical and statistical methods. Another inversion technique was proposed by Haboudane et al. [18] and Atzberger et al. [35]. They developed VIs–LAI relationships calibrated on synthetic data generated by RTM (e.g., so-called predictive equations) for model inversion. This technique combines the advantages of physical and statistical approaches, being characterized by simplicity of application and robustness in LAI retrieval. However, in previous studies, the $PE_{physical}$ were evaluated on a small number of crops (maize, wheat, soybeans, or grasslands), preventing the identification of "universal" relationships between LAI and VIs. In operational situations, a universal algorithm is more functional than crop-specific relations for retrieving different crops' LAI [36]. Therefore, the use of a higher number of crops must be investigated to identify an algorithm based on $PE_{physical}$ that achieves reliable accuracy on average, regardless of the type of canopy structure.

In this context, the main objective of this study was to evaluate the accuracy and the transferability of $PE_{physical}$ calibrated on data simulated by PROSAIL in LAI retrieval of multiple crops by comparing them with some of the most common LAI retrieval methods, such as (i) empirical models based on VIs and in situ data, (ii) empirical correlations found in scientific literature, (iii) the PROSAIL model inversion based on LUT, and (iv) the PROSAIL model inversion based on NNET models. Moreover, the overall aim of this study

was to apply a cost-effective strategy for local validation of different LAI retrieval methods in a specific area.

2. Materials and Methods

2.1. Study Area

The test sites are located in the Po plain of the Emilia-Romagna region, Northern Italy, which is characterised by a temperate climate corresponding to the "Cfa" group according to the Köppen–Geiger climate classification [37] with an average annual precipitation of 700 mm and an average annual temperature of 14 °C. Field measurements were conducted at three different test sites and during three growing seasons: at the Acqua Campus agricultural test field, a Canale Emiliano-Romagnolo (CER) research centre in the municipality of Budrio (Bologna) in 2019 and 2020; in two farms near Ravenna in 2020 and 2021; in two fields near Piacenza in 2021 (Figure 1).

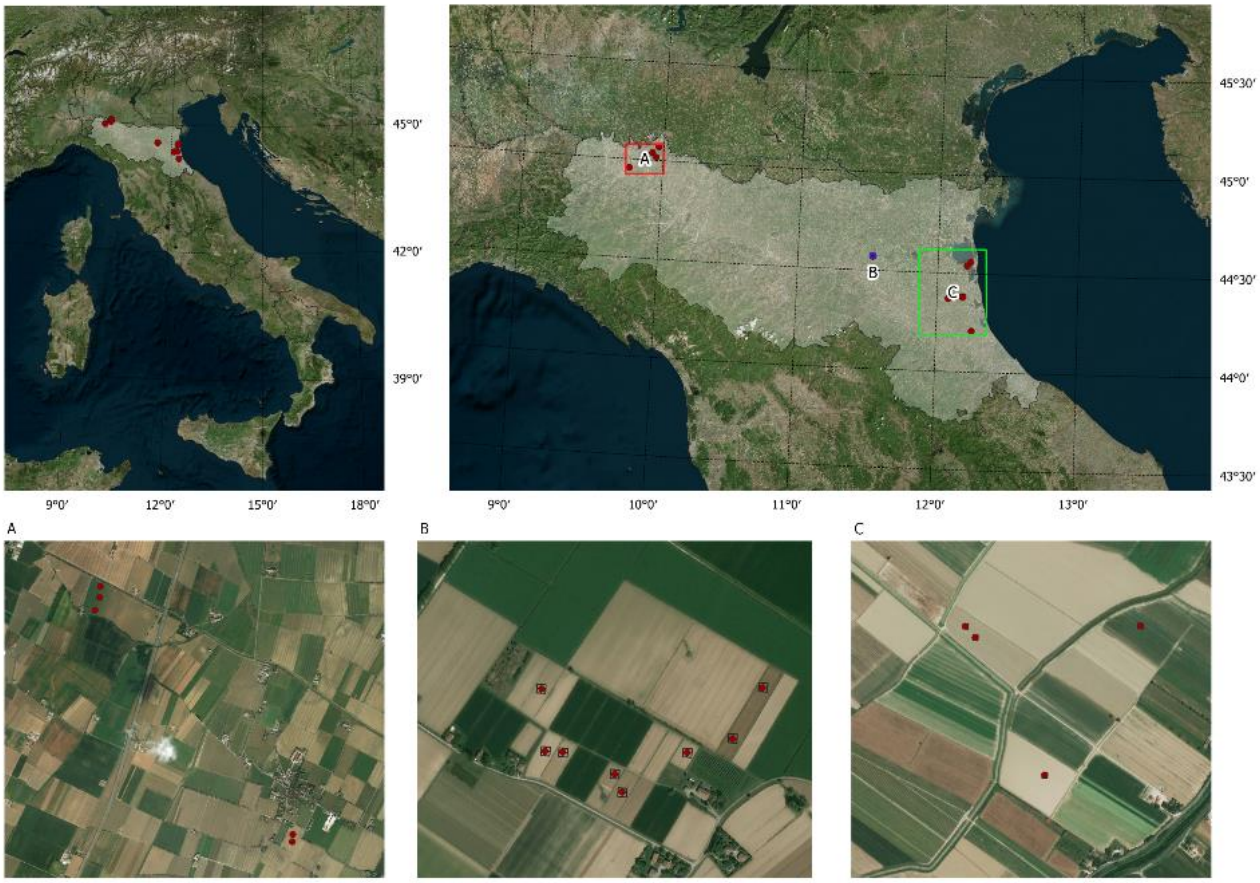

Figure 1. Study area. The study was carried out in an agricultural region located in the North of Italy: (**A**) Piacenza test site (**B**); Budrio test site; and (**C**) Ravenna test site. All the test sites are in the Emilia-Romagna region (grey shading in the top-right image).

2.2. Field Measurement Protocol

Ground-based LAI measurements were collected at each test site. The size of the sampling units was based on an Elementary Sampling Unit (ESU) to better correlate the data with satellite resolution. Each ESU corresponded to a Sentinel-2 pixel (20 × 20 m) and included three fixed-pattern secondary sampling units (SSUs) along the diagonal axis for each of the four pixels 10 × 10 m constituting the ESU (Figure 2).

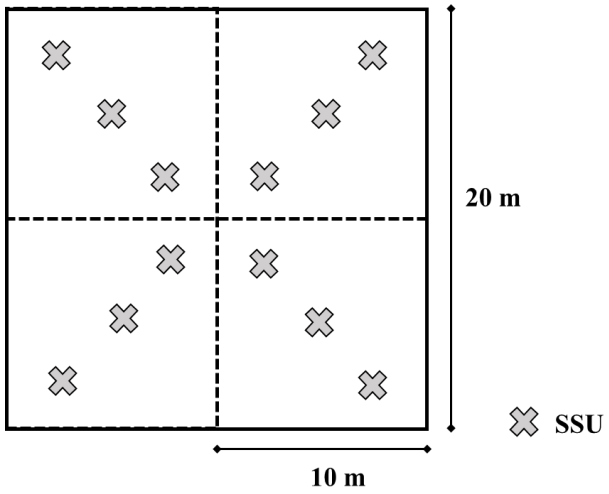

Figure 2. Field measurement protocol for each Elementary Sampling Unit (ESU).

A total of 40 elementary sampling units (ESUs) were chosen in the centre of the monitored fields, maintaining a minimum distance of 10 m from the field boundaries. In situ LAI measurements were recorded within the SSUs by using an AccuPAR LP-80® portable photosynthetically active radiation ceptometer to measure LAI non-destructively. For each ESU, the LAI values of the twelve SSUs were averaged and the average LAI value per ESU was obtained. The vertices and centre of the ESUs were geolocated using a GPS, providing an accuracy of less than 1 m for subsequent matching of the average LAI estimate with the corresponding Sentinel-2 reflectance data. In total, 106 LAI data from 40 ESUs were taken evaluating six different crops: Garlic (*Allium sativum* L.), Tomato (*Solanum lycopersicum* L.), Potato (*Solanum tuberosum* L.), Maize (*Zea mays* L.), Onion (*Allium cepa* L.), and Spinach (*Spinacia oleracea* L.), as shown in Table 1, which summarises the characteristics of the three test sites used in this study. The dataset covers a wide range of LAI values, i.e., from 0.05 to 7, providing an optimal experimental dataset for evaluating each methodology.

Table 1. Characteristics of the three datasets used in this study.

Test Site	Crop Types	Year	N° ESUs	N° LAI	N° Images	Image Acquisition Dates	Field Measurement Dates
A	Garlic (*Allium sativum* L.)	2021	7	30	7	2021 (19 March, 23 April, 3 May, 28 May, 17 June, 25 June, 7 July)	2021 (22 March, 19 April, 5 May, 28 May, 17 June, 25 June, 7 July)
	Tomato (*Solanum lycopersicum* L.)		3	6			
B	Tomato (*Solanum lycopersicum* L.)	2019	2	6	4	2019 (24 May, 18 June, 8 July, 23 July)	2019 (24 May, 18 June, 8 July, 23 July)
	Potato (*Solanum tuberosum* L.)		2	4			
	Maize (*Zea mays* L.)		2	8			
	Onion (*Allium cepa* L.)		2	8			
	Tomato (*Solanum lycopersicum* L.)	2020	2	6	4	2020 (28 May, 22 June, 22 July, 11 August)	2020 (28 May, 22 June, 22 July, 11 August)
	Potato (*Solanum tuberosum* L.)		2	4			
	Maize (*Zea mays* L.)		2	8			
	Onion (*Allium cepa* L.)		2	6			
C	Spinach (*Spinacia oleracea* L.)	2020	6	8	2	2020 (10 October, 22 October)	2020 (9 October, 19 October)
		2021	8	12	4	2021 (20 April, 3 May, 10 May, 18 May)	2021 (20 April, 4 May, 10 May, 18 May)

2.3. Satellite Data Acquisition and Processing

The Sentinel-2 (S2) mission of the European Space Agency's Copernicus program consists of a pair of satellites launched in 2015 and 2017. Both satellites carry a Multi-

Spectral Imager (MSI) with a swath of 290 km and provide data in 13 spectral bands ranging from the visible and near-infrared to the shortwave infrared region, including four bands at 10 m, six bands at 20 m, and three bands at 60 m spatial resolution [38]. Sentinel-2 provides data every 10 days at the equator with one satellite and five days with two satellites under cloud-free conditions, resulting in 2–3 days at mid-latitudes. Sentinel-2 images at Level 2A were downloaded for free from the Copernicus Open Access Hub website (https://scihub.copernicus.eu/ (accessed on 30 May 2021)). All field campaigns were carried out at days close, with a maximum of five days' difference, to the Sentinel-2 overflight dates over the study area (Table 1).

3. Methods

To evaluate the performance of $PE_{physical}$ in LAI retrieval, its accuracy was compared with the performances achieved by four others LAI retrieval methods (Figure 3): two RTM inversion methods (one based on a LUT and the other on an NNET) and two statistical modelling methods (one based on in situ data and the other based on empirical models found in scientific literature). These methods were chosen since they are the most widely used by the remote sensing community, and a detailed description of each method is provided in the following sections. For $PE_{physical}$ and empirical models (in situ data), both linear and 2nd-order polynomial regression for VIs-LAI relation were tested. The VIs evaluated numbered 21: CIgreen, CIre, EVI, EVI2, GNDVI, greenWDRVI, MSAVI, MTVI2, NDGI43, NDRE, NDVI, NDWI, OSAVI, RDVI, rededgeWDRVI, RI, SR, TRBI, TVI, VARIrededge, and WDRVI3. Table 2 displays the equations of each tested VI.

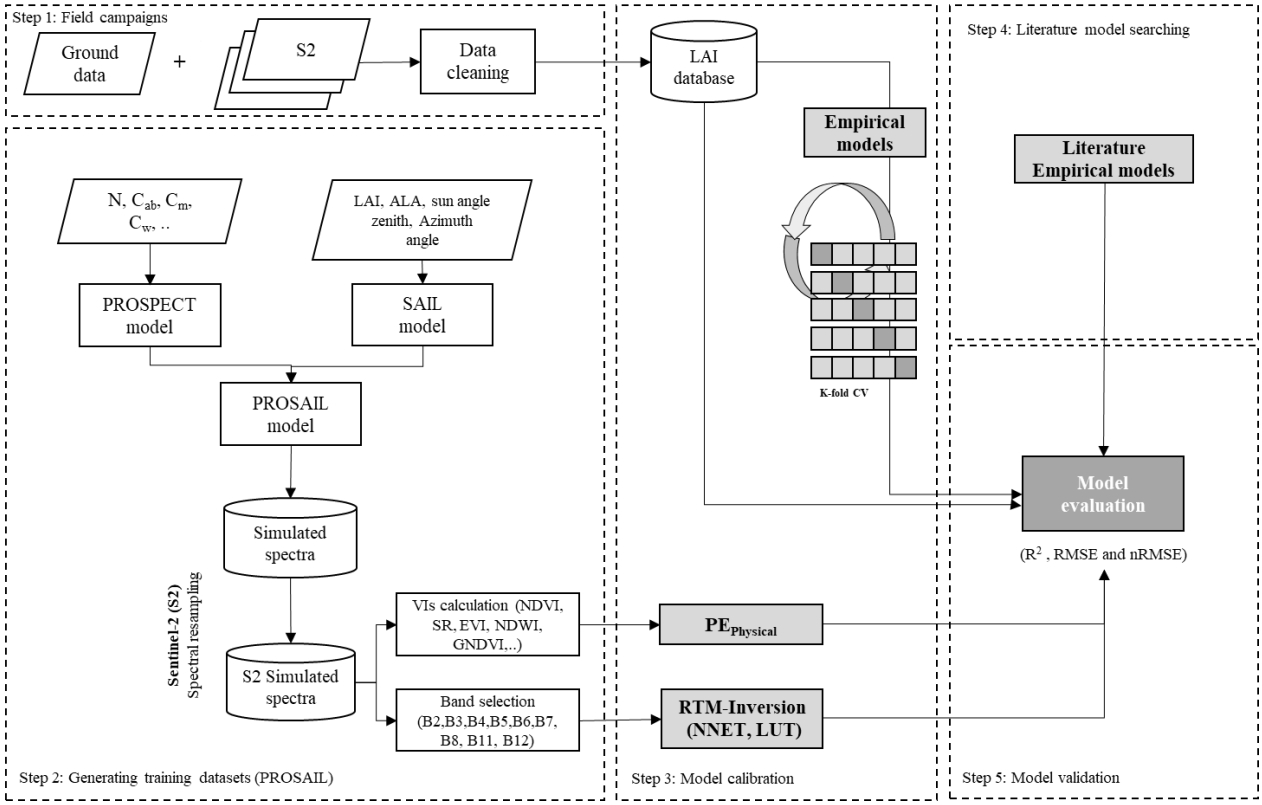

Figure 3. The general framework of the work: Step 1: field campaigns; Step 2: generating training datasets using PROSAIL; Step 3: model calibration (for the empirical model); Step 4: literature model searching, and Step 5: model accuracy assessment.

Table 2. List of the vegetation indices evaluated for the retrieval of Leaf Area Index. Sentinel-2 bands used are the blue (B2), green (B3), red (B4), red-edge 1 (B5), red-edge 3 (B7), NIR (B8), and SWIR (B11).

VIs	Equation	Reference
CI_{green}	$\frac{B8}{B3} - 1$	[39]
CI_{re}	$\frac{B8}{B5} - 1$	[39]
EVI	$2.5 \cdot \left(\frac{(B8 - B4)}{1 + B8 + 6 \cdot B4 - 7.5 \cdot B2} \right)$	[40]
EVI2	$2.4 \cdot \left(\frac{B8 - B4}{1 + B8 + B4} \right)$	[41]
GNDVI	$\frac{(B8 - B3)}{(B8 + B3)}$	[42]
greenWDRVI	$\frac{(0.1 \cdot B8 - B3)}{(0.1 \cdot B8 + B3)} + \frac{(1 - 0.1)}{(1 + 0.1)}$	[43]
MSAVI	$\frac{(2 \cdot B8 + 1 - \sqrt{(2 \cdot B8 + 1)^2 - (8 \cdot (B8 - B4))}}{2}$	[44]
MTVI2	$1.5 \cdot \left(\frac{(1.2 \cdot (B8 - B3) - 2.5 \cdot (B4 - B3))}{\sqrt{\left((2 \cdot B8 + 1)^2 - \left(\left(6 \cdot B8 - 5 \cdot \sqrt{B4} - 0.5\right)\right)\right)}} \right)$	[18]
NDRE	$\frac{(B8 - B5)}{(B8 + B5)}$	[42]
NDVI	$\frac{(B8 - B4)}{(B8 + B4)}$	[45]
NDWI	$\frac{(B8 - B11)}{(B8 + B11)}$	[46]
OSAVI	$(1 + 0.16) \cdot \frac{(B8 - B4)}{(B8 + B4 + 0.16)}$	[47]
RDVI	$\frac{(B8 - B4)}{(B8 + B4)^{0.5}}$	[48]
rededgeWDRVI	$\frac{(0.1 \cdot B8 - B5)}{(0.1 \cdot B8 + B5)} + \frac{(1 - 0.1)}{(1 + 0.1)}$	[43]
RI	$\frac{(B4 - B3)}{(B4 + B3)}$	[49]
SR	$\frac{B8}{B4}$	[50]
TRBI	$\frac{(B3 + B4)}{B8}$	[51]
WDRVI3	$\frac{(0.2 \cdot B8 - B4)}{(0.2 \cdot B8 + B4)} + \frac{(1 - 0.2)}{(1 + 0.2)}$	[52]
NDGI43	$\frac{(B7 - B4)}{(B7 + B4)}$	[49]
TVI	$0.5 \cdot (120 \cdot (B6 - B3) - 200 \cdot (B4 - B3))$	[48]
VARIrededge	$\frac{(B5 - B4)}{(B5 + B4)}$	[39]

3.1. Empirical and Empirical Literature Models

In situ LAI data (n = 106) were sequentially regressed (linearly and polynomially) against 21 VIs to determine which achieved the best performance. A cross-validation strategy based on the k-fold technique was used to ensure more robust results [53] and the available dataset was divided into k = 5 subsets. From these k subsets, one subset was selected as the calibration dataset ($n \simeq 21$), and the remaining k-1 subsets were used for model validation ($n \simeq 85$). The cross-validation process was then repeated k times, with each k subsets used as the calibration dataset. Thus, all the in-situ data were used for both calibration and validation.

In addition to statistical approaches based on empirical models calibrated to in situ data, relationships found in scientific literature were evaluated. The relationships evaluated were taken from the leading scientific articles studying the relationship between vegetation indices and LAI. Table S1 displays the equation for estimating LAI found in scientific literature [36,39,48,52,54–61].

3.2. PROSAIL Model

The PROSAIL radiative transfer model [62] was selected for the physically based canopy parameter retrieval methods. The PROSAIL is a coupled model of the leaf model PROSPECT-5 [63] and the canopy model SAILH [27] that simulates the top of canopy bidirectional reflectance from 400 to 2500 nm. The leaf model simulates leaf reflectance and transmittance considering the mesophyll structural parameter (N), leaf chlorophyll (C_{ab}), dry matter (C_m), and water (C_w) contents. C_w is tied to the dry matter content ($C_w = C_m \times C_{wREL}/(1 - C_{wREL})$), assuming that green leaves have a relative water content (C_{wREL}) varying within a relatively small range [64]. The SAILH model is characterised by the Average Leaf Inclination Angle (ALIA), the Leaf Area Index (LAI) and the hot-spot parameter (hspot). Additionally, information about viewing geometries, i.e., sun and sensor (observer) zenith angles (SZA and OZA, respectively) as well as the relative azimuth angle between both (rAA), must be provided by the users. The values of the input parameters (C_{ab}, LAI, etc.) were selected based on existing literature focused on the studied crops [65] The PROSAIL inputs (parameter combinations) and outputs (spectral reflectance) were used to generate a synthetic database. The synthetic database generated included 278,400 parameter combinations following the ranges (minimum and maximum) and the step of the parameters summarised in Table 3. PROSAIL model as implemented in the "hsdar" R package [66] was used to simulate the canopy reflectance. This study tested three inversion approaches (LUT, NNET and $PE_{physical}$). All PROSAIL inversion methods use the same input combination to ensure perfect comparability. In both cases, the synthetic dataset generated via PROSAIL was spectrally resampled according to the Sentinel-2 response functions [67,68]. For LUT and NNET inversion, all the spectral bands at 10 m and at 20 m of spatial resolutions (except for B8a spectral band) were used, while for $PE_{physical}$, 21 VIs (from one to one) were calculated on a synthetic dataset.

Table 3. Ranges of input parameters for the PROSAIL model.

Parameter	Abbreviation	Unit	Distribution	Min Value	Max Value	Step
Leaf parameters						
Leaf structure parameter	N	-	-	1.5		
Dry matter content	C_m	g cm^{-2}	Uniform	0.001	0.02	0.005
Relative water content	C_{wREL}	%	Uniform	70	90	5
Leaf chlorophyll content	Cab	µg cm^{-2}	Uniform	40	80	10
Canopy parameters						
Leaf Area Index	LAI	m^2 m^{-2}	Uniform	0	7	0.25
Average leaf inclination angle	ALIA	Deg	Uniform	40	70	10
Hot spot parameter	hot	m m^{-1}	-	0.5		
Sun zenith angle	SZA/θs	deg				
Observer zenith angle	OZA/θv	deg	According to actual conditions during data/image acquisition			
Relative azimuth angle	rAA/øSV	deg				
Soil parameter						
Soil brightness	Scale	-	-	0.5	1.5	0.5

3.2.1. PROSAIL Inversion Using Predictive Equations ($PE_{physical}$)

Predictive equations ($PE_{physical}$) inversion method [14,35,69,70] were fitted using the LAI values of the synthetic database (a small part of the synthetic database was used) and each VI by linear and second-order polynomial regressions. The same 21 VIs used in the empirical models were used for $PE_{physical}$ modelling.

3.2.2. The Look-Up Table Inversion Method

The look-up table (LUT) was sorted using the cost function based on root mean square error (RMSE) to find the solution to the inverse problem for the measured canopy reflectance [30,71]. The $RMSE_r$ cost function (Equation (1)), between the measured reflectance and the simulated reflectance found in the LUT, was calculated as follows:

$$RMSE_r = \sqrt{\frac{\sum_{i=1}^{n}\left(R_{measured_i} - R_{simulated_i}\right)^2}{n}} \quad (1)$$

where n is the number of spectral bands used in the present work, $R_{measured_i}$ is the reflectance at spectral band i measured by the Sentinel-2, and $R_{simulated_i}$ is the simulated reflectance at spectral band i in the LUT. The solution was determined using the mean value of LAI corresponding to the best 100 solutions (i.e., having the smallest sorted *RMSEr*).

3.2.3. PROSAIL Inversion Using NNET

A simple "feed-forward" neural network (NNET) with a single hidden layer (input layer, one hidden layer, and one output layer) was used to invert the PROSAIL database. Part of the parameter combinations and the simulated spectral reflectance of the synthetic database were used to train the NNET for LAI retrieval. The NNET was trained using the "*caret*" R package [72]. There are two steps to train the Neural Network: (i) a feed-forward iteration to compute the network's output; (ii) a back-propagation learning rule to minimise the error between predicted outputs and input training values. The training dataset was used to optimise the number of units in the hidden layer (size) and decay of the NNET, while the error of the test dataset was monitored during the training process. To optimise the hyper-parameters of the NNET, a searching grid was applied. The number of hidden units was tuned for each value between 1 and 50 [72]. Weight decay was tuned between 0.1 and 10 with step of 1 increment.

3.3. Model Evaluation

The performance of the LAI retrieval methods was evaluated using the coefficient of determination (R^2)—(2), Root Mean Square Error (*RMSE*)—(3) and normalised *RMSE* (*nRMSE*)—(4), which is the *RMSE* divided by the range of the reference measurements between the in situ data values.

$$R^2 = \frac{\left(\sum_{i=1}^{n}(y_i - \overline{y}_i)\left(f_i - \overline{f}_i\right)\right)^2}{\sum_{i=1}^{n}(y_i - \overline{y}_i)^2 \sum_{i=1}^{n}\left(f_i - \overline{f}_i\right)^2} \quad (2)$$

$$RMSE = \sqrt{\frac{1}{n}\sum_{i=1}^{n}(y_i - f_i)^2} \quad (3)$$

$$nRMSE = \frac{RMSE}{y_{i,max} - y_{i,min}} \quad (4)$$

where n (i = 1, 2, . . . , n) is the number of samples used to test each Leaf Area Index (LAI) technique, y_i is the observed LAI, $\overline{y}_i$ is the corresponding mean value, f_i is the predicted LAI and $\overline{f}_i$ is the corresponding mean value. The closer R^2 is to 1, the higher the retrieval performance of the model is. Small *nRMSE* (%) and *RMSE* values indicate less discrepancy within observed and predicted measurement.

4. Results

4.1. $PE_{physical}$ vs. RTM-Inversion Methods

Results obtained with the physical approaches are summarised in Figure 4 and Table S2. The performance of the predictive equation ($PE_{physical}$) was compared against the other two inversion methods (NNET and LUT) based on a PROSAIL synthetic database. Inversion

by NNET gave good accuracy for the estimation of LAI (R^2 = 0.73, RMSE = 0.86 m^2 m^{-2} and nRMSE = 10.53 %). In the $PE_{physical}$, the best performing VI for LAI retrieval was the OSAVI (R^2 = 0.77, RMSE = 0.84 m^2 m^{-2} and nRMSE = 10.34 %), followed by MSAVI and EVI2. The best $PE_{physical}$ (the one based on OSAVI) was more accurate than both RTM inversion based on NNET and LUT (Figure 4) with an RMSE of 0.84 m^2 m^{-2} ($PE_{physical}$) vs. 0.86 m^2 m^{-2} and 0.94 m^2 m^{-2} (NNET and LUT, respectively).

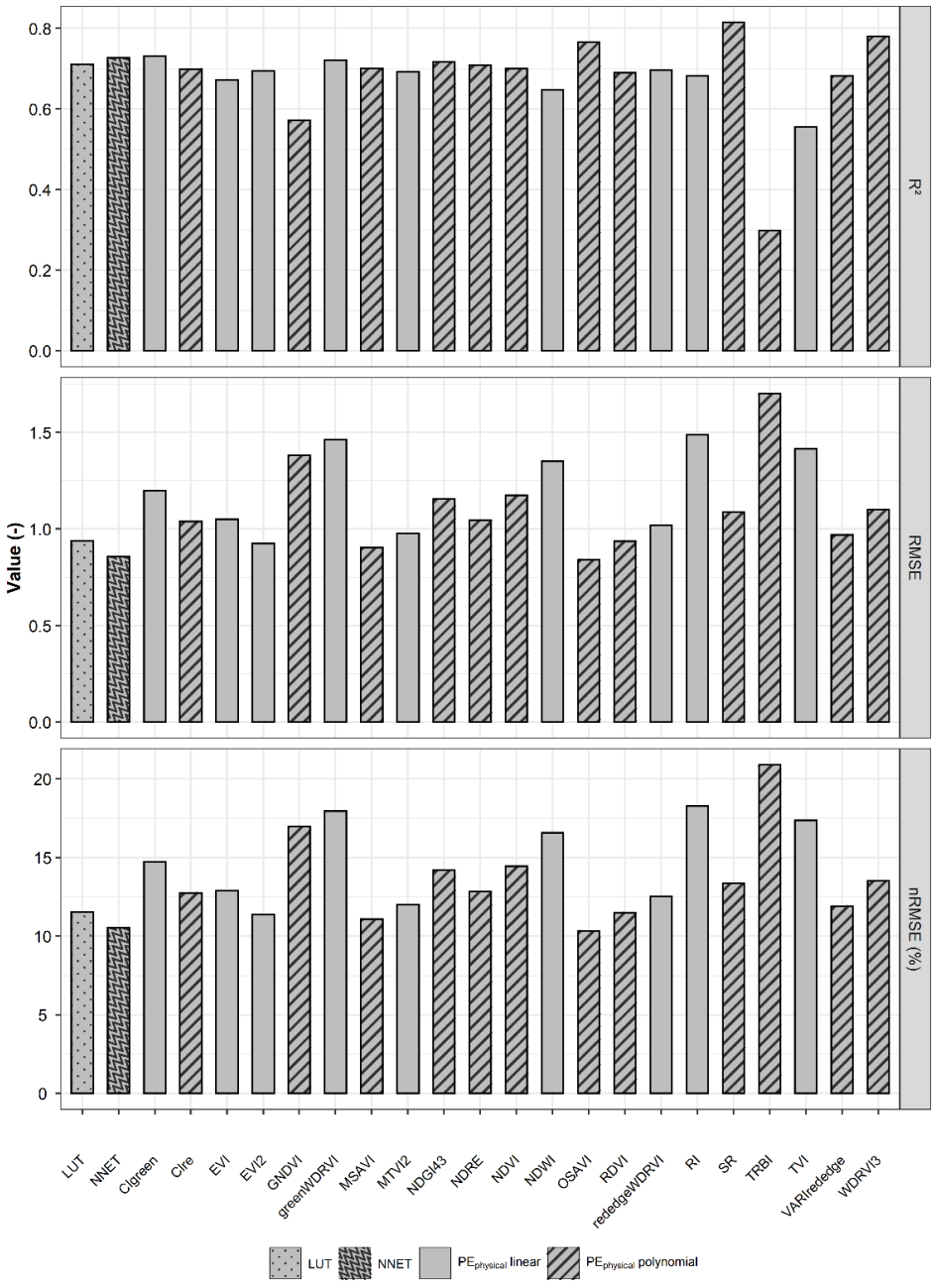

Figure 4. R^2, RMSE and nRMSE (%) obtained between field measured and retrieved LAI from physical approaches (LUT, NNET, and $PE_{physical}$).

4.2. $PE_{physical}$ vs. Empirical and Empirical Literature Models

The best-performing VIs of $PE_{physical}$ were compared (Figure 5 and Table S3) to the values of R^2, RMSE and nRMSE (%) achieved by the same VIs for empirical and literature models (for this method only the best performance of the VIs between several literature models evaluated was reported). The accuracy achieved by the OSAVI polynomial

of the PE (RMSE = 0.84 m^2 m^{-2}) was similar to the OSAVI polynomial of the empirical (RMSE = 0.79 m^2 m^{-2}) while the OSAVI of the literature achieved the worst performance (RMSE = 2.40 m^2 m^{-2}). The SR and WDRVI3 displayed higher performance with an RMSE of 0.71 m^2 m^{-2} and 0.78 m^2 m^{-2} for SR and with an RMSE of 0.76 m^2 m^{-2} and 0.77 m^2 m^{-2} for WDRVI3 for empirical and literature models, respectively.

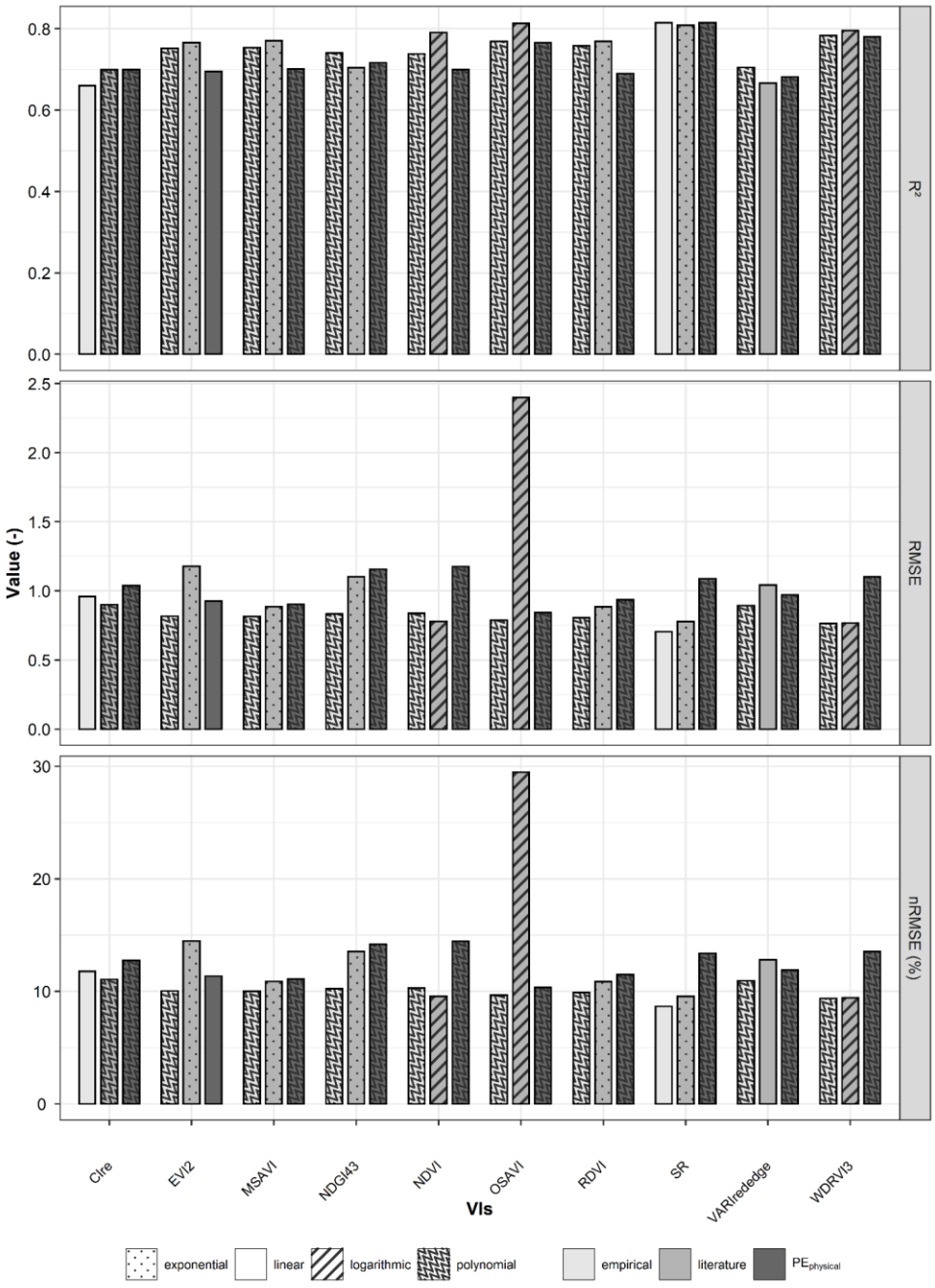

Figure 5. R^2, RMSE and nRMSE (%) obtained between field measured and retrieved LAI from empirical, empirical literature models compared to $PE_{physical}$.

4.3. Crop Specific Differences

Overall, the method based on linear empirical models (i.e., SR) provided the lowest values of RMSE (0.71 m^2 m^{-2}) and the highest value of R^2 (0.81). Moreover, it provided the best performance in terms of nRMSE (8.66%). In contrast, the RTM-inversion method based on NNET obtained the lowest performance with 0.86 m^2 m^{-2}, 10.53%, and 0.73 of

RMSE, nRMSE, and R^2, respectively. However, by analysing the scatterplots between the measured and retrieved LAI (Figure 6) of the best models for each evaluated method (i.e., empirical, literature, RTM-inversion and $PE_{physical}$), the retrieval performance appeared to vary among different crops (Figure 6), which exhibited different canopy structures.

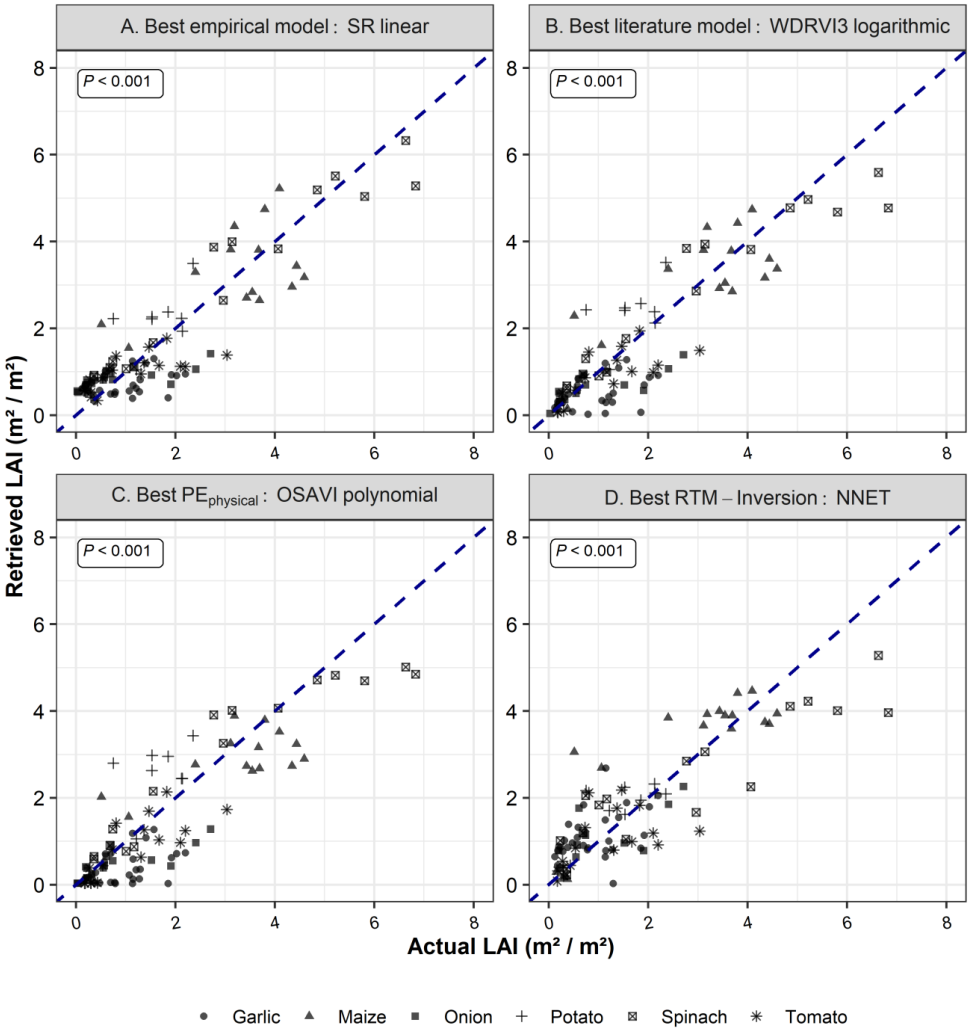

Figure 6. Retrieved versus measured LAI using the best statistical approaches and physical approaches (**A**) best empirical model: linear regression between LAI and SR; (**B**) best literature model: WDRVI3 (i.e., [52]); (**C**) Best $PE_{physical}$ model: based on OSAVI-second-order polynomial fitting; (**D**) best RTM-inversion using PROSAIL: NNET.

In general, the methods for LAI retrieval showed the best performance for spinach with nRMSE ranging from 8.36% (Empirical model SR Linear) to 16.13% (NNET-inversion) and the worst performance for potato with nRMSE ranging from 37.58% (NNET-inversion) to 70.17% ($PE_{physical}$ OSAVI polynomial). When compared to the other three methods, $PE_{physical}$ (OSAVI) achieved a similar accuracy in LAI retrieval for spinach, maize, and tomato, but instead, its accuracy was low concerning the potato (Figure 7).

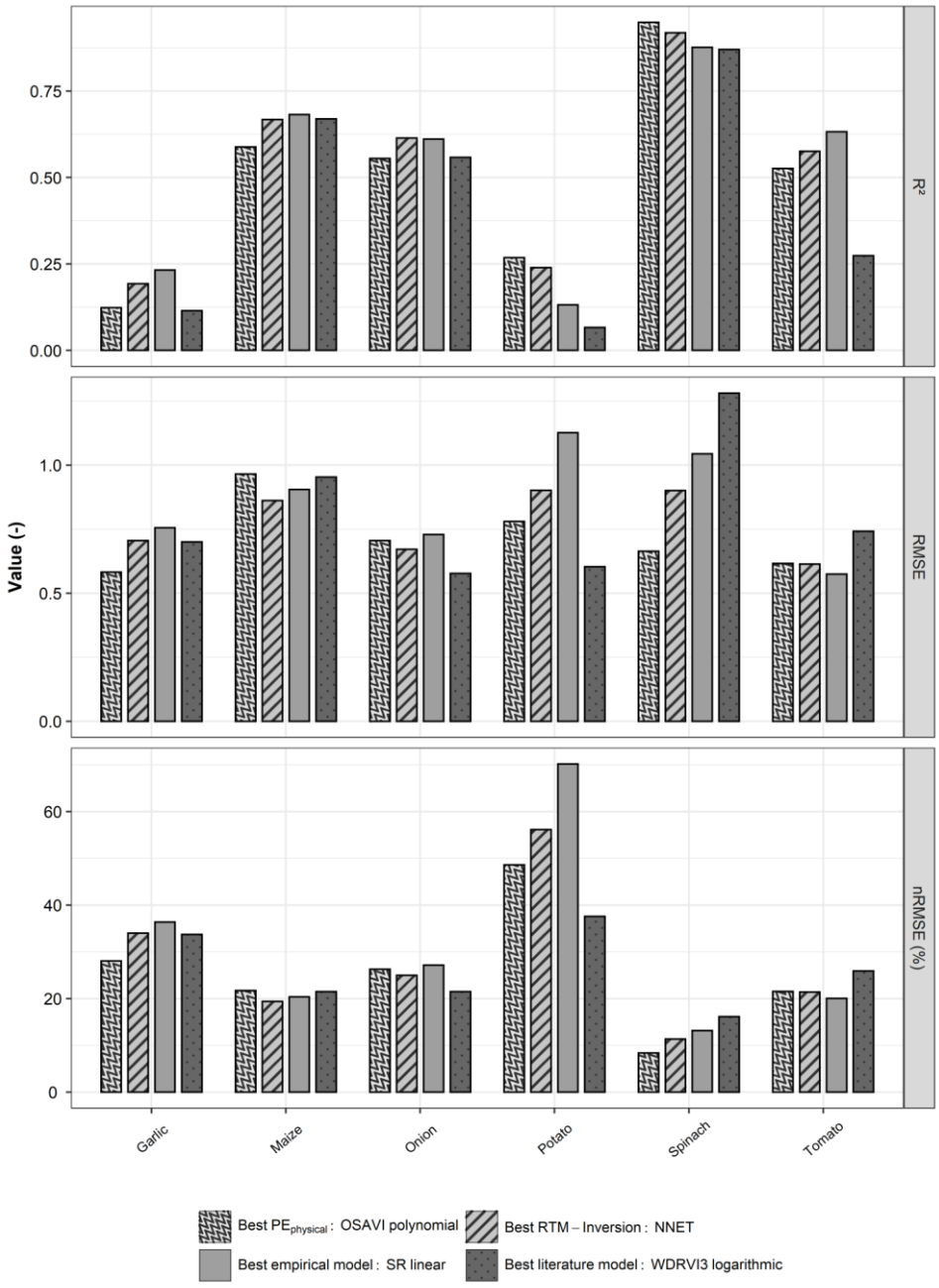

Figure 7. R^2, RMSE, and nRMSE (%) of the best model one for each LAI retrieval method according to different crops (Garlic, Maize, Onion, Potato, Spinach, and Tomato). Best empirical model: linear regression between LAI and SR; best RTM-inversion: NNET; best literature model: WDRVI3-based model provided by [52]; best $PE_{physical}$ model: based on OSAVI-second-order polynomial fitting.

5. Discussion

In this study, the predictive equations ($PE_{physical}$) method were compared with different methodologies (empirical models, empirical literature models, and RTM inversion based on NNET and LUT) to evaluate the accuracy and transferability in Leaf Area Index (LAI) retrieval on six of the main irrigated crops in Northern Italy (i.e., garlic, maize, onion, potato, spinach, tomato). The results were analysed by computing R^2, RMSE, and nRMSE (%) values considering all crops together and for each specific crop. $PE_{physical}$ is an interesting RTM inversion alternative to traditional techniques such as LUT and machine learning algorithms (e.g., NNET) for LAI retrieval because of its ability to combine a physical approach and ease of use. $PE_{physical}$ is calibrated on synthetically generated databases

where VIs are calculated and fitted with LAI by linear or polynomial models. This method produced models with similar accuracy using OSAVI, MSAVI, and EVI2 than the inversion methods based on NNET and LUT. In particular, in this study $PE_{physical}$ with OSAVI, MSAVI, and EVI2 was more accurate than LUT, while $PE_{physical}$ with OSAVI alone was more accurate than NNET. These results do not confirm what has been reported in previous studies. In fact, applying $PE_{physical}$ to HyMap hyperspectral data over grasslands produced models with significantly lower accuracy than inversion with LUT [35]. In general, RTM inversion based on NNET and LUT provided acceptable results overall, demonstrating that radiative transfer model inversion can achieve comparable performance to statistical approaches, which are generally always better performing, as reported in previous studies [35,66,67,73–75]). However, RTM approaches require a fine parameterisation process that is quite complex and labour intensive, especially if several crops are being studied. An important difference between the RTM inversion based on NNET and LUT and the other methods used in this work consists in the number of spectral bands involved in LAI retrieval. RTM inversion based on NNET and LUT considers the entire spectral signature of each pixel, while the other methods rely on only two or more spectral bands. This implies a reduction in the computing resources required paired with a reduction in noise sensitivity, ensuring greater robustness, generalisation, and reproducibility. In the context of RTM inversion approaches, the results achieved by $PE_{physical}$, which partially uses physical knowledge incorporated in the RTM, encourage the use of this method. This is due to its high accuracy and extremely fast and straightforward inversion after calibration thanks to the use of VIs from the straightforward synthetic database.

Overall, without analysing the results for individual crops, the best linear empirical model achieved the highest performance for LAI retrieval. Among the statistical approaches, models derived from the literature [36,49,59] have also demonstrated satisfactory performance. Most notably, the models published by Nguy-Robertson et al. [52] achieved very high levels of accuracy and only slightly lower compared with the empirical models developed in this study. However, the models from literature were only validated on the dataset collected at the test sites adding confidence compared to the empirical models, for which part of the dataset had to be used for calibration. The SR and WDRVI3 showed the highest performance both for empirical and literature models. The SR and WDRVI3 vegetation indices equation uses only NIR and red bands. These bands are also used for calculating OSAVI, MSAVI, and EVI2 which showed the highest performance in the $PE_{physical}$ method. The use of these bands only for accurate LAI retrieval contrasts claims reported in previous studies where vegetation indices that do not include the red-edge band are more crop specific [36]. In fact, it has been reported in other studies [49,66] that Sentinel-2 bands located in the red-edge region are key bands for LAI retrieval [66,76–78].

When analysing the performance of the methods for individual crops, it was observed that the best (low nRMSE) and worst (high nRMSE) performances were achieved for spinach and potato, respectively. All methods achieved excellent performance for spinach while NNET-based RTM inversion achieved higher performance for potato than other methods. $PE_{physical}$ (OSAVI) in comparison with other methods achieved a good accuracy in LAI retrieval for spinach, maize, and tomato, while low accuracy for potato. This was probably due to the smaller dimension of the dataset related to potato, but generally the accuracy of LAI retrieval was lower for all row crops (potato, garlic, onion and tomato) compared with maize or spinach. This could also be related to soil effect that could affect the spectral data.

6. Conclusions

The aim of this study was to apply a cost-effective strategy for local validation of different LAI retrieval methods in a specific area. The predictive equations' ($PE_{physical}$) accuracy for LAI retrieval was evaluated in this study by comparison of empirical models, empirical literature models, and two RTM inversions based on NNET and LUT, respectively. LAI data of six irrigated crops in Northern Italy (i.e., Garlic, Maize, Onion, Potato,

Spinach, and Tomato) were collected in different years and locations in order to compare the transferability of these methods. The results obtained suggested that $PE_{physical}$ accurately retrieved the LAI of the crops evaluated (except for the potato). The best performance of $PE_{physical}$ was achieved by the OSAVI index (RMSE = 0.84 m^2 m^{-2}), and this method was more accurate than NNET and LUT inversion methods for LAI retrieval. LAI retrieval through $PE_{physical}$ enabled achieving excellent results using even two spectral bands (i.e., NIR and red) compared with RTM inversion based on NNET and LUT, which use more spectral bands. $PE_{physical}$ methods also achieved performance akin to that of empirical and empirical literature models, indicating that $PE_{physical}$ could be employed for the retrieval ofto retrieve LAI to monitor crop growth and improve efficiency in agricultural practices. In fact, the use of $PE_{physical}$ enables to combine of the merits of statistical and physical approaches by integrating the simplicity of use and ease of implementation of the empirical models with the ability to use (even if partially) the physical knowledge and transferability typical of radiative transfer models.

Supplementary Materials: The following supporting information can be downloaded at: https://www.mdpi.com/article/10.3390/agronomy12112835/s1, Supplementary Material Table S1. Literature relationships evaluated for LAI retrieval. Equation and reference are presented; Supplementary Material Table S2. R^2, RMSE and nRMSE (%) obtained between field measured and retrieved LAI from physical approaches (LUT, NNET and $PE_{physical}$); Supplementary Material Table S3. R^2, RMSE and nRMSE (%) obtained between field measured and retrieved LAI from empirical, empirical literature models compared to $PE_{physical}$.

Author Contributions: M.C. (Michele Croci): conceptualisation, data curation, methodology, investigation, formal analysis, writing—original draft. G.I.: data curation, investigation. G.A.: investigation, editing. T.L.: data curation, investigation. A.M.: investigation. F.V.: investigation. M.V.: investigation. M.C. (Michele Colauzzi): investigation. S.A. (Stefano Anconelli): funding acquisition, project administration. S.A. (Stefano Amaducci): conceptualisation, funding acquisition, supervision, review and editing. All authors have read and agreed to the published version of the manuscript.

Funding: The authors would like to acknowledge the support of Project "Protocolli Operativi Scalabili per l'agricoltura di precisione-POSITIVE"-CUP: D41F18000080009. One of the authors (MC) would like to acknowledge support from the Emilia-Romagna Region DGR n. 769 del 21/05/2018 co-financed by the European Social Fund (ESF) POR-FESR 2014-2020.

Data Availability Statement: The data that support the findings of this work are available from the corresponding author upon reasonable request.

Conflicts of Interest: The authors declare no conflict of interest. The funders had no role in the design of the study, in the collection, analyses, or interpretation of data, in the writing of the manuscript, or in the decision to publish the result.

References

1. Brisco, B.; Brown, R.J.; Hirose, T.; McNairn, H.; Staenz, K. Precision Agriculture and the Role of Remote Sensing: A Review. *Can. J. Remote Sens.* **1998**, *24*, 315–327. [CrossRef]
2. Wang, K.; Franklin, S.E.; Guo, X.; Cattet, M. Remote Sensing of Ecology, Biodiversity and Conservation: A Review from the Perspective of Remote Sensing Specialists. *Sensors* **2010**, *10*, 9647–9667. [CrossRef] [PubMed]
3. Peng, Y.; Zhu, T.; Li, Y.; Dai, C.; Fang, S.; Gong, Y.; Wu, X.; Zhu, R.; Liu, K. Remote Prediction of Yield Based on LAI Estimation in Oilseed Rape under Different Planting Methods and Nitrogen Fertilizer Applications. *Agric. For. Meteorol.* **2019**, *271*, 116–125. [CrossRef]
4. Defourny, P.; Bontemps, S.; Bellemans, N.; Cara, C.; Dedieu, G.; Guzzonato, E.; Hagolle, O.; Inglada, J.; Nicola, L.; Rabaute, T.; et al. Near Real-Time Agriculture Monitoring at National Scale at Parcel Resolution: Performance Assessment of the Sen2-Agri Automated System in Various Cropping Systems around the World. *Remote Sens. Environ.* **2019**, *221*, 551–568. [CrossRef]
5. Xie, Y.; Sha, Z.; Yu, M. Remote Sensing Imagery in Vegetation Mapping: A Review. *J. Plant Ecol.* **2008**, *1*, 9–23. [CrossRef]
6. Pu, R.; Gong, P.; Biging, G.S.; Larrieu, M.R. Extraction of Red Edge Optical Parameters from Hyperion Data for Estimation of Forest Leaf Area Index. *IEEE Trans. Geosci. Remote Sens.* **2003**, *41*, 916–921.
7. Turner, D.P.; Cohen, W.B.; Kennedy, R.E.; Fassnacht, K.S.; Briggs, J.M. Relationships between Leaf Area Index and Landsat TM Spectral Vegetation Indices across Three Temperate Zone Sites. *Remote Sens. Environ.* **1999**, *70*, 52–68. [CrossRef]

8. Jégo, G.; Pattey, E.; Liu, J. Using Leaf Area Index, Retrieved from Optical Imagery, in the STICS Crop Model for Predicting Yield and Biomass of Field Crops. *Field Crop. Res.* **2012**, *131*, 63–74. [CrossRef]
9. Gilardelli, C.; Stella, T.; Confalonieri, R.; Ranghetti, L.; Campos-Taberner, M.; García-Haro, F.J.; Boschetti, M. Downscaling Rice Yield Simulation at Sub-Field Scale Using Remotely Sensed LAI Data. *Eur. J. Agron.* **2019**, *103*, 108–116. [CrossRef]
10. Houlès, V.; Guérif, M.; Mary, B. Elaboration of a Nitrogen Nutrition Indicator for Winter Wheat Based on Leaf Area Index and Chlorophyll Content for Making Nitrogen Recommendations. *Eur. J. Agron.* **2007**, *27*, 1–11. [CrossRef]
11. Bréda, N.J.J. Ground-Based Measurements of Leaf Area Index: A Review of Methods, Instruments, and Current Controversies. *J. Exp. Bot.* **2003**, *54*, 2403–2417. [CrossRef] [PubMed]
12. Immitzer, M.; Vuolo, F.; Atzberger, C. First Experience with Sentinel-2 Data for Crop and Tree Species Classifications in Central Europe. *Remote Sens.* **2016**, *8*, 166. [CrossRef]
13. Baret, F.; Buis, S. Estimating Canopy Characteristics from Remote Sensing Observations: Review of Methods and Associated Problems. In *Advances in Land Remote Sensing*; Springer: Dordrecht, The Netherlands, 2008; pp. 173–201.
14. Rivera, J.; Verrelst, J.; Delegido, J.; Veroustraete, F.; Moreno, J. On the Semi-Automatic Retrieval of Biophysical Parameters Based on Spectral Index Optimization. *Remote Sens.* **2014**, *6*, 4927–4951. [CrossRef]
15. Houborg, R.; Boegh, E. Mapping Leaf Chlorophyll and Leaf Area Index Using Inverse and Forward Canopy Reflectance Modeling and SPOT Reflectance Data. *Remote Sens. Environ.* **2008**, *112*, 186–202. [CrossRef]
16. Jacquemoud, S.; Baret, F.; Andrieu, B.; Danson, F.M.; Jaggard, K.; Danson, M.; Jaggard, K. Extraction of Vegetation Biophysical Parameters by Inversion of the PROSPECT+SAIL Model on Sugar Beet Canopy Reflectance Data: Application to TM and AVIRIS Sensors. *Remote Sens. Environ.* **1995**, *52*, 163–172. [CrossRef]
17. Verrelst, J.; Camps-Valls, G.; Muñoz-Marí, J.; Rivera, J.P.; Veroustraete, F.; Clevers, J.G.P.W.; Moreno, J. Optical Remote Sensing and the Retrieval of Terrestrial Vegetation Bio-Geophysical Properties—A Review. *ISPRS J. Photogramm. Remote Sens.* **2015**, *108*, 273–290. [CrossRef]
18. Haboudane, D.; Miller, J.R.; Pattey, E.; Zarco-Tejada, P.J.; Strachan, I.B. Hyperspectral Vegetation Indices and Novel Algorithms for Predicting Green LAI of Crop Canopies: Modeling and Validation in the Context of Precision Agriculture. *Remote Sens. Environ.* **2004**, *90*, 337–352. [CrossRef]
19. Khanna, S.; Palacios-Orueta, A.; Whiting, M.L.; Ustin, S.L.; Riaño, D.; Litago, J. Development of Angle Indexes for Soil Moisture Estimation, Dry Matter Detection and Land-Cover Discrimination. *Remote Sens. Environ.* **2007**, *109*, 154–165. [CrossRef]
20. Mutanga Correspond, O.; Skidmore, A.K. Narrow Band Vegetation Indices Overcome the Saturation Problem in Biomass Estimation. *Int. J. Remote Sens.* **2004**, *25*, 3999–4014. [CrossRef]
21. Yu, K.; Li, F.; Gnyp, M.L.; Miao, Y.; Bareth, G.; Chen, X. Remotely Detecting Canopy Nitrogen Concentration and Uptake of Paddy Rice in the Northeast China Plain. *ISPRS J. Photogramm. Remote Sens.* **2013**, *78*, 102–115. [CrossRef]
22. Glenn, E.P.; Huete, A.R.; Nagler, P.L.; Nelson, S.G. Relationship between Remotely-Sensed Vegetation Indices, Canopy Attributes and Plant Physiological Processes: What Vegetation Indices Can and Cannot Tell Us about the Landscape. *Sensors* **2008**, *8*, 2136–2160. [CrossRef] [PubMed]
23. Baret, F.; Guyot, G. Potentials and Limits of Vegetation Indices for LAI and APAR Assessment. *Remote Sens. Environ.* **1991**, *35*, 161–173. [CrossRef]
24. Vuolo, F.; Neugebauer, N.; Bolognesi, S.F.; Atzberger, C.; D'Urso, G. Estimation of Leaf Area Index Using DEIMOS-1 Data: Application and Transferability of a Semi-Empirical Relationship between Two Agricultural Areas. *Remote Sens.* **2013**, *5*, 1274–1291. [CrossRef]
25. Atzberger, C.; Darvishzadeh, R.; Schlerf, M.; le Maire, G. Suitability and Adaptation of PROSAIL Radiative Transfer Model for Hyperspectral Grassland Studies. *Remote Sens. Lett.* **2013**, *4*, 55–64. [CrossRef]
26. Jacquemoud, S.; Baret, F. PROSPECT: A Model of Leaf Optical Properties Spectra. Remote Sens. *Remote Sens. Environ.* **1990**, *34*, 75–91. [CrossRef]
27. Verhoef, W. Light Scattering by Leaf Layers with Application to Canopy Reflectance Modeling: The SAIL Model. *Remote Sens. Environ.* **1984**, *16*, 125–141. [CrossRef]
28. Kimes, D.S.; Knyazikhin, Y.; Privette, J.L.; Abuelgasim, A.A.; Gao, F. Inversion Methods for Physically-based Models. *Remote Sens. Rev.* **2000**, *18*, 381–439. [CrossRef]
29. Weiss, M.; Baret, F. Evaluation of Canopy Biophysical Variable Retrieval Performances from the Accumulation of Large Swath Satellite Data. *Remote Sens. Environ.* **1999**, *70*, 293–306. [CrossRef]
30. Darvishzadeh, R.; Skidmore, A.; Schlerf, M.; Atzberger, C. Inversion of a Radiative Transfer Model for Estimating Vegetation LAI and Chlorophyll in a Heterogeneous Grassland. *Remote Sens. Environ.* **2008**, *112*, 2592–2604. [CrossRef]
31. Rivera, J.P.; Verrelst, J.; Leonenko, G.; Moreno, J. Multiple Cost Functions and Regularization Options for Improved Retrieval of Leaf Chlorophyll Content and LAI through Inversion of the PROSAIL Model. *Remote Sens.* **2013**, *5*, 3280–3304. [CrossRef]
32. Weiss, M.; Baret, F.; Myneni, R.B.; Pragnère, A.; Knyazikhin, Y. Investigation of a Model Inversion Technique to Estimate Canopy Biophysical Variables from Spectral and Directional Reflectance Data. *Agronomie* **2000**, *20*, 3–22. [CrossRef]
33. Schlerf, M.; Atzberger, C. Inversion of a Forest Reflectance Model to Estimate Structural Canopy Variables from Hyperspectral Remote Sensing Data. *Remote Sens. Environ.* **2006**, *100*, 281–294. [CrossRef]

34. Verger, A.; Baret, F.; Camacho, F. Optimal Modalities for Radiative Transfer-Neural Network Estimation of Canopy Biophysical Characteristics: Evaluation over an Agricultural Area with CHRIS/PROBA Observations. *Remote Sens. Environ.* **2011**, *115*, 415–426. [CrossRef]
35. Atzberger, C.; Darvishzadeh, R.; Immitzer, M.; Schlerf, M.; Skidmore, A.; le Maire, G. Comparative Analysis of Different Retrieval Methods for Mapping Grassland Leaf Area Index Using Airborne Imaging Spectroscopy. *Int. J. Appl. Earth Obs. Geoinf.* **2015**, *43*, 19–31. [CrossRef]
36. Nguy-Robertson, A.L.; Peng, Y.; Gitelson, A.A.; Arkebauer, T.J.; Pimstein, A.; Herrmann, I.; Karnieli, A.; Rundquist, D.C.; Bonfil, D.J. Estimating Green LAI in Four Crops: Potential of Determining Optimal Spectral Bands for a Universal Algorithm. *Agric. For. Meteorol.* **2014**, *192–193*, 140–148. [CrossRef]
37. Peel, M.C.; Finlayson, B.L.; McMahon, T.A. Updated World Map of the Köppen-Geiger Climate Classification. *Hydrol. Earth Syst. Sci. Discuss.* **2007**, *4*, 439–473. [CrossRef]
38. Drusch, M.; del Bello, U.; Carlier, S.; Colin, O.; Fernandez, V.; Gascon, F.; Hoersch, B.; Isola, C.; Laberinti, P.; Martimort, P.; et al. Sentinel-2: ESA's Optical High-Resolution Mission for GMES Operational Services. *Remote Sens. Environ.* **2012**, *120*, 25–36. [CrossRef]
39. Gitelson, A.A.; Viña, A.; Arkebauer, T.J.; Rundquist, D.C.; Keydan, G.; Leavitt, B. Remote Estimation of Leaf Area Index and Green Leaf Biomass in Maize Canopies. *Geophys. Res. Lett.* **2003**, *30*, 52. [CrossRef]
40. Huete, A.; Didan, K.; Miura, T.; Rodriguez, E.P.; Gao, X.; Ferreira, L.G. Overview of the Radiometric and Biophysical Performance of the MODIS Vegetation Indices. *Remote Sens. Environ.* **2002**, *83*, 195–213. [CrossRef]
41. Jiang, Z.; Huete, A.; Didan, K.; Miura, T. Development of a Two-Band Enhanced Vegetation Index without a Blue Band. *Remote Sens. Environ.* **2008**, *112*, 3833–3845. [CrossRef]
42. Gitelson, A.; Merzlyak, M.N. Quantitative Estimation of Chlorophyll-a Using Reflectance Spectra: Experiments with Autumn Chestnut and Maple Leaves. *J. Photochem. Photobiol. B* **1994**, *22*, 247–252. [CrossRef]
43. Gitelson, A.A. Wide Dynamic Range Vegetation Index for Remote Quantification of Biophysical Characteristics of Vegetation. *J. Plant Physiol.* **2004**, *161*, 165–173. [CrossRef] [PubMed]
44. Qi, J.; Chehbouni, A.; Huete, A.R.; Kerr, Y.H.; Sorooshian, S. A Modified Soil Adjusted Vegetation Index. *Remote Sens. Environ.* **1994**, *48*, 119–126. [CrossRef]
45. Rouse, J.W.; Haas, R.H.; Schell, J.A.; Deering, D.W. Monitoring Vegetation Systems in the Great Plains with ERTS. In Proceedings of the 3rd ERTS Symposium, Washington, DC, USA, 10–14 December 1973; NASA SP-351. Nasa Special Publication: Washington, DC, USA, 1973; pp. 309–317.
46. Gao, B.-C. NDWI—A Normalized Difference Water Index for Remote Sensing of Vegetation Liquid Water from Space. *Remote Sens. Environ.* **1996**, *58*, 257–266. [CrossRef]
47. Rondeaux, G.; Steven, M.; Baret, F. Optimization of Soil-Adjusted Vegetation Indices. *Remote Sens. Environ.* **1996**, *55*, 95–107. [CrossRef]
48. Broge, N.H.; Leblanc, E. Comparing Prediction Power and Stability of Broadband and Hyperspectral Vegetation Indices for Estimation of Green Leaf Area Index and Canopy Chlorophyll Density. *Remote Sens. Environ.* **2001**, *76*, 156–172. [CrossRef]
49. Pasqualotto, N.; Delegido, J.; van Wittenberghe, S.; Rinaldi, M.; Moreno, J. Multi-Crop Green LAI Estimation with a New Simple Sentinel-2 LAI Index (SeLI). *Sensors* **2019**, *19*, 904. [CrossRef]
50. Birth, G.S.; McVey, G.R. Measuring the Color of Growing Turf with a Reflectance Spectrophotometer 1. *Agron. J.* **1968**, *60*, 640–643. [CrossRef]
51. Vincini, M.; Frazzi, E.; D'Alessio, P. A Broad-Band Leaf Chlorophyll Vegetation Index at the Canopy Scale. *Precis. Agric.* **2008**, *9*, 303–319. [CrossRef]
52. Nguy-Robertson, A.; Gitelson, A.; Peng, Y.; Viña, A.; Arkebauer, T.; Rundquist, D. Green Leaf Area Index Estimation in Maize and Soybean: Combining Vegetation Indices to Achieve Maximal Sensitivity. *Agron. J.* **2012**, *104*, 1336–1347. [CrossRef]
53. Snee, R.D. Validation of Regression Models: Methods and Examples. *Technometrics* **1977**, *19*, 415–428. [CrossRef]
54. Clevers, J.G.P.W.; Kooistra, L.; van den Brande, M.M.M. Using Sentinel-2 Data for Retrieving LAI and Leaf and Canopy Chlorophyll Content of a Potato Crop. *Remote Sens.* **2017**, *9*, 405. [CrossRef]
55. Kang, Y.; Özdoğan, M.; Zipper, S.C.; Román, M.O.; Walker, J.; Hong, S.Y.; Marshall, M.; Magliulo, V.; Moreno, J.; Alonso, L.; et al. How Universal Is the Relationship between Remotely Sensed Vegetation Indices and Crop Leaf Area Index? A Global Assessment. *Remote Sens.* **2016**, *8*, 597. [CrossRef] [PubMed]
56. Delegido, J.; Verrelst, J.; Rivera, J.P.; Ruiz-Verdú, A.; Moreno, J. Brown and Green LAI Mapping through Spectral Indices. *ITC J.* **2015**, *35*, 350–358. [CrossRef]
57. Rinaldi, M.; Ruggieri, S.; Garofalo, P.; Vonella, A.V.; Satalino, G.; Soldo, P. Leaf Area Index Retrieval Using High Resolution Remote Sensing Data. *Ital. J. Agron.* **2010**, *5*, 155–166. [CrossRef]
58. Papadavid, G. Mapping Potato Crop Height and Leaf Area Index through Vegetation Indices Using Remote Sensing in Cyprus. *J. Appl. Remote Sens.* **2011**, *5*, 53526. [CrossRef]
59. Viña, A.; Gitelson, A.A.; Nguy-Robertson, A.L.; Peng, Y. Comparison of Different Vegetation Indices for the Remote Assessment of Green Leaf Area Index of Crops. *Remote Sens. Environ.* **2011**, *115*, 3468–3478. [CrossRef]
60. Delegido, J.; Verrelst, J.; Meza, C.M.; Rivera, J.P.; Alonso, L.; Moreno, J. A Red-Edge Spectral Index for Remote Sensing Estimation of Green {LAI} over Agroecosystems. *Eur. J. Agron.* **2013**, *46*, 42–52. [CrossRef]

61. Li, M.; Chu, R.; Yu, Q.; Islam, A.; Chou, S.; Shen, S. Evaluating Structural, Chlorophyll-Based and Photochemical Indices to Detect Summer Maize Responses to Continuous Water Stress. *Water* **2018**, *10*, 500. [CrossRef]
62. Jacquemoud, S.; Verhoef, W.; Baret, F.; Bacour, C.; Zarco-Tejada, P.J.; Asner, G.P.; François, C.; Ustin, S.L. PROSPECT + SAIL Models: A Review of Use for Vegetation Characterization. *Remote Sens. Environ.* **2009**, *113*, S56–S66. [CrossRef]
63. Feret, J.-B.; François, C.; Asner, G.P.; Gitelson, A.A.; Martin, R.E.; Bidel, L.P.R.; Ustin, S.L.; le Maire, G.; Jacquemoud, S. PROSPECT-4 and 5: Advances in the Leaf Optical Properties Model Separating Photosynthetic Pigments. *Remote Sens. Environ.* **2008**, *112*, 3030–3043. [CrossRef]
64. Baret, F.; Hagolle, O.; Geiger, B.; Bicheron, P.; Miras, B.; Huc, M.; Berthelot, B.; Niño, F.; Weiss, M.; Samain, O.; et al. LAI, fAPAR and FCover CYCLOPES Global Products Derived from VEGETATION. *Remote Sens. Environ.* **2007**, *110*, 275–286. [CrossRef]
65. Duveiller, G.; Weiss, M.; Baret, F.; Defourny, P. Retrieving Wheat Green Area Index during the Growing Season from Optical Time Series Measurements Based on Neural Network Radiative Transfer Inversion. *Remote Sens. Environ.* **2011**, *115*, 887–896. [CrossRef]
66. Lehnert, L.W.; Meyer, H.; Obermeier, W.A.; Silva, B.; Regeling, B.; Bendix, J. Hyperspectral Data Analysis in R: The hsdar Package. *J. Stat. Softw.* **2019**, *89*, 1–23. [CrossRef]
67. Squeri, C.; Gatti, M.; Garavani, A.; Vercesi, A.; Buzzi, M.; Croci, M.; Calegari, F.; Vincini, M.; Poni, S. Ground Truthing and Physiological Validation of Vis-NIR Spectral Indices for Early Diagnosis of Nitrogen Deficiency in Cv. Barbera (*Vitis vinifera* L.) Grapevines. *Agronomy* **2019**, *9*, 864. [CrossRef]
68. Xie, Q.; Dash, J.; Huete, A.; Jiang, A.; Yin, G.; Ding, Y.; Peng, D.; Hall, C.C.; Brown, L.; Shi, Y.; et al. Retrieval of Crop Biophysical Parameters from Sentinel-2 Remote Sensing Imagery. *Int. J. Appl. Earth Obs. Geoinf.* **2019**, *80*, 187–195. [CrossRef]
69. le Maire, G.; Marsden, C.; Nouvellon, Y.; Stape, J.-L.; Ponzoni, F. Calibration of a Species-Specific Spectral Vegetation Index for Leaf Area Index (LAI) Monitoring: Example with MODIS Reflectance Time-Series on Eucalyptus Plantations. *Remote Sens.* **2012**, *4*, 3766–3780. [CrossRef]
70. le Maire, G.; François, C.; Soudani, K.; Berveiller, D.; Pontailler, J.Y.; Bréda, N.; Genet, H.; Davi, H.; Dufrêne, E.; Lemaire, G.; et al. Calibration and Validation of Hyperspectral Indices for the Estimation of Broadleaved Forest Leaf Chlorophyll Content, Leaf Mass per Area, Leaf Area Index and Leaf Canopy Biomass. *Remote Sens. Environ.* **2008**, *112*, 3846–3864. [CrossRef]
71. Sehgal, V.K.; Chakraborty, D.; Sahoo, R.N. Inversion of Radiative Transfer Model for Retrieval of Wheat Biophysical Parameters from Broadband Reflectance Measurements. *Inf. Process. Agric.* **2016**, *3*, 107–118. [CrossRef]
72. Kuhn, M.; Johnson, K. *Applied Predictive Modeling*, 1st ed.; Springer: New York, NY, USA, 2019.
73. Gemmell, F.; Varjo, J.; Strandstrom, M.; Kuusk, A. Comparison of Measured Boreal Forest Characteristics with Estimates from TM Data and Limited Ancillary Information Using Reflectance Model Inversion. *Remote Sens. Environ.* **2002**, *81*, 365–377. [CrossRef]
74. le Maire, G.; Marsden, C.; Verhoef, W.; Ponzoni, F.J.; lo Seen, D.; Bégué, A.; Stape, J.-L.; Nouvellon, Y. Leaf Area Index Estimation with MODIS Reflectance Time Series and Model Inversion during Full Rotations of Eucalyptus Plantations. *Remote Sens. Environ.* **2011**, *115*, 586–599. [CrossRef]
75. Atzberger, C.; Guérif, M.; Baret, F.; Werner, W. Comparative Analysis of Three Chemometric Techniques for the Spectroradiometric Assessment of Canopy Chlorophyll Content in Winter Wheat. *Comput. Electron. Agric.* **2010**, *73*, 165–173. [CrossRef]
76. Delegido, J.; Verrelst, J.; Alonso, L.; Moreno, J. Evaluation of Sentinel-2 Red-Edge Bands for Empirical Estimation of Green LAI and Chlorophyll Content. *Sensors* **2011**, *11*, 7063–7081. [CrossRef] [PubMed]
77. Clevers, J.G.P.W.; Gitelson, A.A. Remote Estimation of Crop and Grass Chlorophyll and Nitrogen Content Using Red-Edge Bands on Sentinel-2 and -3. *ITC J.* **2013**, *23*, 344–351. [CrossRef]
78. Cui, Z.; Kerekes, J.P. Potential of Red Edge Spectral Bands in Future Landsat Satellites on Agroecosystem Canopy Green Leaf Area Index Retrieval. *Remote Sens.* **2018**, *10*, 1458. [CrossRef]